Neuroscience 185 (2011) 125–134

INCREASED EXPRESSION OF ACYL-COENZYME A: CHOLESTEROL ACYLTRANSFERASE-1 AND ELEVATED CHOLESTERYL ESTERS IN THE HIPPOCAMPUS AFTER EXCITOTOXIC INJURY

J.-H. KIM,[a] S.-M. EE,[a] J. JITTIWAT,[b] E.-S. ONG,[c] A. A. FAROOQUI,[d] A. M. JENNER[e] AND W.-Y. ONG[a,f]*

[a]*Department of Anatomy, National University of Singapore, Singapore 119260*

[b]*Department of Physiology, Khon Kaen University, Thailand*

[c]*Department of Epidemiology and Public Health, National University of Singapore, Singapore 119260*

[d]*Department of Molecular and Cellular Biochemistry, The Ohio State University, USA*

[e]*Illawara Health and Medical Research Institute, University of Wollongong, NSW 2522, Australia*

[f]*Neurobiology and Ageing Research Programme, National University of Singapore, Singapore 119260*

Abstract—Significant increases in levels of cholesterol and cholesterol oxidation products are detected in the hippocampus undergoing degeneration after excitotoxicity induced by the potent glutamate analog, kainate (KA), but until now, it is unclear whether the cholesterol is in the free or esterified form. The present study was carried out to examine the expression of the enzyme involved in cholesteryl ester biosynthesis, acyl-coenzyme A: cholesterol acyltransferase (ACAT) and cholesteryl esters after KA excitotoxicity. A 1000-fold greater basal mRNA level of ACAT1 than ACAT2 was detected in the normal brain. ACAT1 mRNA and protein were upregulated in the hippocampus at 1 and 2 weeks after KA injections, at a time of glial reaction. Immunohistochemistry showed ACAT1 labeling of oligodendrocytes in the white matter and axon terminals in hippocampal CA fields of normal rats, and loss of staining in neurons but increased immunoreactivity of oligodendrocytes, in areas affected by KA. Gas chromatography-mass spectrometry analyses confirmed previous observations of a marked increase in level of total cholesterol and cholesterol oxidation products, whilst nuclear magnetic resonance spectroscopy showed significant increases in cholesteryl ester species in the degenerating hippocampus. Upregulation of ACAT1 expression was detected in OLN93 oligodendrocytes after KA treatment, and increased expression was prevented by an antioxidant or free radical scavenger *in vitro*. This suggests that ACAT1 expression may be induced by oxidative stress. Together, our results show elevated ACAT1 expression and increased cholesteryl esters after KA excitotoxicity. Further studies are necessary to determine a possible role of ACAT1 in acute and chronic neurodegenerative diseases. © 2011 IBRO. Published by Elsevier Ltd. All rights reserved.

*Correspondence to: W.-Y. Ong, Department of Anatomy, National University of Singapore, Singapore 119260. Tel: +65-65163662; fax: +65-67787643.
E-mail address: wei_yi_ong@nuhs.edu.sg (W.-Y. Ong).

Abbreviations: ACAT, acyl-coenzyme A: cholesterol acyltransferase; CNPase, 2′,3′-cyclic nucleotide 3′-phosphodiesterase; KA, kainate; NMR, nuclear magnetic resonance; PBS, phosphate-buffered saline.

Key words: cholesterol, cholesteryl esters, neuroinflammation, cholesterol oxidation products, oxidative stress, ACAT1.

Cholesteryl esters are formed by cholesterol and fatty acyl coenzyme A such as arachidonoyl-coenzyme A, and hydrolyzed back to cholesterol continuously, forming the cholesterol/cholesteryl ester cycle (Brown et al., 1980). Hydrolysis of cholesteryl esters provides cholesterol and fatty acids for membrane formation and maintenance, lipoprotein trafficking, lipid detoxification, evaporation barriers, and fuel in times of stress or nutrient deprivation (Turkish and Sturley, 2009). On the other hand, overproduction of cholesteryl esters may be associated with the pathology of obesity, atherosclerosis (Leon et al., 2005; Puglielli et al., 2001; Zhao et al., 2009), and Alzheimer's disease (AD) (Puglielli et al., 2001). Cholesterol is crucial for the integrity of the cell membrane, cell signaling, and gene transcription (Bjorkhem and Meaney, 2004) and disruption in homeostasis is observed in neurodegenerative diseases such as Niemann-Pick C disease, multiple sclerosis (Leoni et al., 2005), and AD (Adibhatla and Hatcher, 2008).

The equilibrium between free and esterified cholesterol is controlled by acyl-coenzyme A: cholesterol acyltransferase (ACAT), an integral membrane protein localized to the endoplasmic reticulum (ER) (Chang et al., 2009). Two isoforms of ACAT, ACAT1 and ACAT2 have been identified in neural and non-neural tissues (Rudel et al., 2001). ACAT1 is a 56 kDa protein present in the brain, liver, adrenal glands, and macrophages (Lee et al., 1998). ACAT2 is mainly expressed in hepatocytes and intestinal mucosal cells (Rudel et al., 2001). ACAT not only plays a role in the reesterification process of cholesterol (Zhang et al., 2003) but also acts as a cholesterol sensor, and expression is induced by increased cholesterol concentrations (Brown and Jessup, 2009). Use of ACAT inhibitors has been explored in the treatment of atherosclerosis (Alegret et al., 2004; Leon et al., 2005) and models of AD (Hull et al., 2006; Huttunen and Kovacs, 2008). ACAT is reported to modulate Aβ formation through control of free cholesterol and cholesteryl ester levels (Cordy et al., 2006).

Increased levels of cholesterol and cholesterol oxidation products (COPs) have been observed in rat hippocampus after excitotoxic injury induced by the potent glutamate analog, kainate (KA) (He et al., 2006; Kim et al., 2009; Ong et al., 2003, 2010b). This is a model of spinal cord injury, head injury, stroke, and neurodegenerative diseases. The hippocampus is one of the most vulnerable brain regions to

0306-4522/11 $ - see front matter
doi:10.1016/j.neuroscience.2011.04.018

KA, which causes neuronal cell loss in cornu ammonis 1 (CA1) and CA3 pyramidal cells and interneurons of the dentate hilus (Ben-Ari, 1985; Nadler et al., 1978). Increased cholesterol and COPs may enhance exocytosis in surviving neurons resulting in propagation of excitotoxic injury (Ma et al., 2010; Zhang et al., 2009). Thus far however, it is unclear whether increased cholesterol after neuronal injury is in the free or esterified form. The present study was carried out, to elucidate the expression of ACAT isoforms in the normal brain and after KA lesions. The levels of free, esterified, and total cholesterol were also determined in the lesioned hippocampus.

EXPERIMENTAL PROCEDURES

Kainate injection

Adult male Wistar rats weighing 200 g each were purchased from Centre for Animal Resources (CARE) of the National University of Singapore. They were anaesthetized by ketamine and xylazine cocktail (prepared with 7.5 ml ketamine (75 mg/kg), 5 ml xylazine (10 mg/kg), and 7.5 ml sterile water) and KA (Tocris Bioscience, MO, USA). 1 μl of 1 mg/ml was i.c.v. injected into the right lateral ventricle through a small craniotomy as previously described (Kim and Ong, 2009). The animals were assessed according to the Racine scale of seizure severity (Racine, 1972) and found to have scores of at least 3 out of 5. Rats were deeply anesthetized and sacrificed at 1 day, 1 week, and 2 weeks after injection as described in the experiments below. All procedures involving animals were approved by the Institutional Animal Care and Use Committee of the National University of Singapore.

RT-PCR analyses

Twenty rats were used for this portion of the study, consisting of untreated controls, and animals injected with KA and sacrificed 1 day, 1 week, and 2 weeks after injection (five rats per group). The lesioned right hippocampi were quickly removed and immersed in RNAlater® (Ambion, TX, USA), snap frozen in liquid nitrogen, and kept at −80 °C till analyses. Total RNA was extracted and isolated using TRizol reagent (Invitrogen, CA, USA) according to the manufacturer's protocol. RNeasy® Mini Kit (Qiagen, Inc., CA, USA) was used to purify the RNA. The samples were then reverse transcribed using High-Capacity cDNA Reverse Transcription Kits (Applied Biosystems, CA, USA). Reaction conditions were 25 °C for 10 min, 37 °C for 120 min and 85 °C for 5 s. Real-time PCR amplification was then carried out in the 7500 Real time PCR system using TaqMan® Universal PCR Master Mix (Applied Biosystems). ACAT1, ACAT2, and β-actin probes were used according to the manufacturers' instructions (Applied Biosystems). The PCR conditions were: an initial incubation of 50 °C for 2 min and 95 °C for 10 min followed by 40 cycles of 95 °C for 15 s and 60 °C for 1 min. All reactions were carried out in triplicate. The threshold cycle, CT, which correlates inversely with the levels of target mRNA, was measured as the number of cycles at which the reporter fluorescence emission exceeds the preset threshold level. The amplified transcripts were quantified using the comparative CT method (Livak and Schmittgen, 2001), with the formula for relative fold change$=2^{-\Delta\Delta CT}$. The mean was calculated and possible significant differences between KA injected and control hippocampal specimens were analyzed using one-way ANOVA with Bonferroni's multiple comparison post-hoc test. $P<0.05$ was considered significant.

Western blot analyses

Twelve rats were used for this portion of the study, consisting of untreated controls, and animals injected with KA and sacrificed 1 day, 1 week, and 2 weeks after injection (three rats per group). The hippocampus was harvested and homogenized in 10 volumes of ice-cold buffer containing 0.32 M sucrose, 4 mM Tris–HCl, pH 7.4, 1 mM EDTA, and 0.25 mM dithiothreitol. After centrifugation at 1000 g for 10 min, the supernatant was collected and protein concentrations in the preparation were measured using the Bio-Rad protein assay kit (Bio-Rad Laboratories, CA, USA). Total proteins (40 μg) were resolved in 10% sodium dodecyl sulfate (SDS) polyacrylamide gels under reducing conditions and electrotransferred to a polyvinylidene difluoride (PVDF) membrane (Amersham Pharmacia Biotech, Little Chalfont, UK). Non-specific binding sites on the PVDF membrane were blocked by incubation with 5% non-fat milk for 1 h. The PVDF membrane was then incubated overnight with rabbit polyclonal antibody to ACAT1 (Cayman, MI, USA, 1:500 dilution in Tris–buffered saline (TBS] at 4 °C. After washing with 0.1% Tween-20 in TBS, the membrane was incubated with horseradish peroxidase conjugated anti-rabbit immunoglobulin IgG (1:2000 dilution) (Amersham) for 1 h at room temperature. The protein was visualized with an enhanced chemiluminescence kit (PiPCe, Rockford, IL, USA). Loading controls were carried out by incubating the blots at 50 °C for 30 min with stripping buffer (100 mM 2-mercaptoethanol, 2% SDS, and 62.5 mM Tris–hydrochloride, pH 6.7), followed by reprobing with a mouse monoclonal antibody to β-actin (Sigma-Aldrich, MO, USA; diluted 1:10,000 in TTBS) and horseradish peroxidase-conjugated anti-mouse IgG (Pierce, Rockford, IL, USA, 1:2000 in TTBS). Exposed films containing blots were scanned and the densities of the bands measured using Gel-Pro Analyzer 3.1 program (Media Cybernetics, Silver Spring, MD, USA). The densities of the ACAT1 bands were normalized against those of β-actin, and the mean ratios calculated. Possible significant differences between the values from the KA-injected and control rats were analyzed using one-way ANOVA with Bonferroni's multiple comparison post-hoc test. $P<0.05$ was considered significant.

Immunoperoxidase labeling

Three untreated control rats and three 1 week post-KA injected rats were used for this portion of the study. The rats were deeply anesthetized and perfused through the left cardiac ventricle with a solution of 4% paraformaldehyde in 0.1 M phosphate buffer (pH 7.4). The fixed brain tissues were removed and sectioned coronally at 100 μm using a Vibrating microtome. The sections were divided for Cresyl Fast Violet (Nissl) and immunohistochemical staining as follows: Sections were washed for 3 h in phosphate-buffered saline (PBS) to remove traces of fixative and then incubated overnight with a rabbit polyclonal antibody to ACAT1 (Cayman, MI, USA, diluted 1:200 in PBS). The sections were then washed three times in PBS and incubated for 1 h at room temperature in a 1:200 dilution of biotinylated horse anti-rabbit IgG (Vector, Burlingame, CA, USA). The sections were reacted for 1 h at room temperature with an avidin-biotinylated horseradish peroxidase complex, and visualized by treatment for 5 min in 0.05% 3,3-diaminobenzidine tetrahydrochloride solution in Tris–buffer containing 0.05% hydrogen peroxide. The color reaction was stopped with several washes of Tris–buffer. Some sections were mounted on glass slides and lightly counterstained with Methyl Green before coverslipping. Control sections were incubated with antigen-absorbed antibody instead of primary antibody (prepared by incubating 200 μg/ml immunizing peptide with ACAT1 antibody overnight).

Double immunofluorescence labeling

Four rats were used for this portion of the study. The rats were injected with KA and sacrificed after 1 week by deep anaesthesia and perfusion through the left cardiac ventricle with a solution of 4% paraformaldehyde in 0.1 M phosphate buffer (pH 7.4). The brains were dissected out, and blocks containing the hippocam-

pus were sectioned at 20 μm using a freezing microtome. The sections were processed for double immunofluorescence staining. They were incubated in a blocking solution composed of 5% donkey serum (Vector) followed by overnight incubation with rabbit polyclonal antibody to ACAT1 (diluted 1:200 in PBS) and mouse antibodies to 2′,3′-cyclic nucleotide 3′-phosphodiesterase (CNPase) (Abcam, UK, diluted 1:200 in PBS), a marker for oligodendrocytes, glial fibrillary acidic protein (GFAP) (Dako, Denmark, diluted 1:1000 in PBS) for astrocytes, and CD11b/c equivalent antibody (OX42) (Millipore, MA, USA, diluted 1:200 in PBS) for microglia. The sections were then washed three times in PBS, and incubated for 1 h at room temperature in 1:200 dilution of FITC-conjugated donkey anti-rabbit IgG, and Cy3-conjugated donkey anti-mouse IgG (both from Millipore). The sections were mounted and examined using an Olympus FluoView FV1000 confocal microscope (Tokyo, Japan). Quantification of double labeling was by counting the number of labeling of marker and number of double-labeled cells. Micrographs of CA3 region of the hippocampus were analyzed from four KA-affected animals. The proportion of double- to single-labeled cells of each marker was then calculated, and possible significant differences analyzed, using one-way ANOVA with Bonferroni's multiple comparison post-hoc test. $P<0.05$ was considered significant.

Electron microscopy

Electron microscopy was carried out by subdissecting some of the immunostained hippocampal sections into smaller portions. These were osmicated, dehydrated in an ascending series of ethanol and acetone, and embedded in Araldite. Thin sections were obtained from the first 5 μm of the sections, mounted on copper grids coated with Formvar, and stained with Lead Citrate. They were viewed using a Jeol 1010EX electron microscope.

Serum cholesterol measurement

Twenty rats were used for this portion of the study. Blood from uninjected controls, and 1 day, 2 weeks, and 1 month post-KA injected rats (five rats per group) was collected via cardiac puncture at the time of sacrifice and centrifuged at 1000 g for 10 min at 4 °C. The upper layer containing cholesterol was separated and transferred to new tubes. A cholesterol detection kit (Biovision, CA, USA) was used to determine serum cholesterol level. Samples were diluted and mixed with assay enzyme. The absorbance of the samples was analyzed at 570 nm. Total cholesterol level was calculated and statistical analyses were carried out using one-way ANOVA with Bonferroni's multiple comparison post-hoc test ($P<0.05$ was considered significant).

Gas chromatography-mass spectrometry analyses of the hippocampus

Twenty-four rats were used for this portion of the study, consisting of untreated controls, and animals injected with KA and sacrificed 1 day, 1 week, and 2 weeks after injection (six rats per group). Hippocampal specimens were homogenized at 4 °C with 0.75 ml PBS and 3.25 ml Folch organic solvent mixture (chloroform/methanol 2:1, containing 0.05% butylated hydroxytoluene [BHT]) (Folch et al., 1957). The homogenates were centrifuged at 1000 g for 10 min at 4 °C. The upper phase was discarded and the lower organic phase carefully transferred to a glass vial and evaporated under a stream of N_2. 0.25 ml of 0.5 M KOH (in 100% methanol) and 0.25 ml of water was added with a mixture of heavy isotopes in 25 μl of ethanol (Kim et al., 2009). All samples were purged with argon gas and closed with a Teflon cap. After gentle mixing, samples were incubated for 15 h at 23 °C in order to measure the total cholesterol and oxysterols. Mixed anion-exchange solid phase extraction columns were pre-conditioned with 2 ml methanol; followed by 2 ml of 40 mM acetate buffer (pH 4.5). 1.5 ml of 0.1 M HCl and 1.5 ml of 80 mM acetic acid were added to the hydrolyzed samples for neutralization. The samples (pH 4.5) were loaded onto the columns, and the columns were washed with 2 ml of 30% methanol/formic acid pH 4.5, followed by 2 ml of hexane and then 2 ml of acetone/hexane (30:70) to elute cholesterol and oxysterols. Eluted samples were evaporated under a stream of nitrogen and derivatized with 25 μl acetonitrile and 25 μl N,O-Bis(trimethylsilyl) trifluoroacetamide+trimethylchlorosilane for an hour at room temperature. Derivatized samples were analyzed using the Agilent 5975 inert XL mass selective detector and Agilent GC in an HPSms column 12 m×0.25 mm diameter (0.25 mm filter thickness) (Kim et al., 2009). Quantification of cholesterol and oxysterols was achieved by relating its peak area of target ion to its corresponding internal standard peak. Statistical analyses was carried out using one-way ANOVA with Bonferroni's multiple comparison post-hoc test ($P<0.05$ was considered significant).

Nuclear magnetic resonance spectroscopy analyses

Twenty-four rats were used for this portion of the study, consisting of untreated controls, and animals injected with KA and sacrificed 1 day, 1 week, and 2 weeks after injection (six rats per group). Lyophilized samples (5–10 mg) were extracted with 0.5 ml of $CHCl_3/CH_3OH$ (3:1). After centrifugation at 12,000 rcf for 5 min,

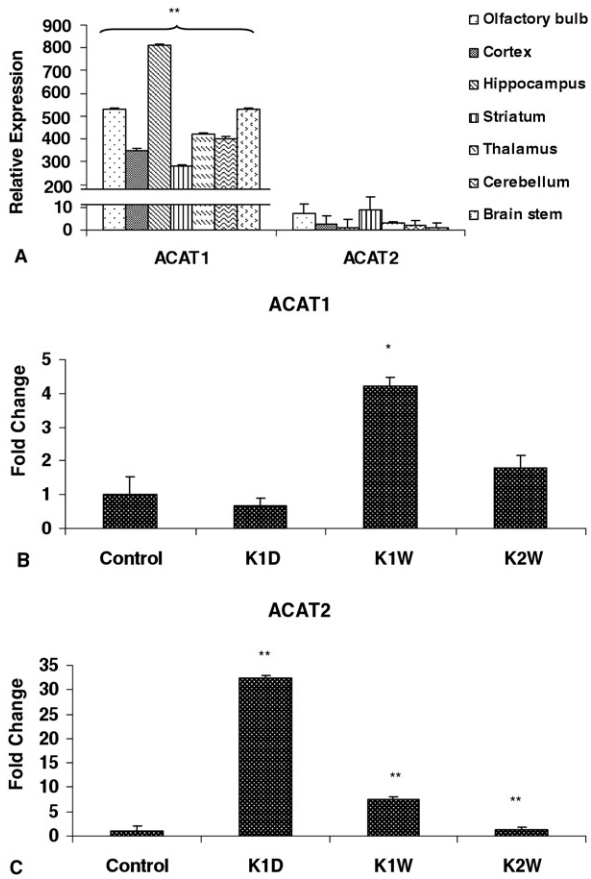

Fig. 1. Real time RT-PCR analyses of ACAT. (A) Normal distribution of ACAT1 and ACAT2 mRNA. The values were normalized to the lowest level of message among the different brain regions, that is, the value for ACAT2 in the hippocampus, to give an indication of relative expression in different parts of the brain. Significantly higher level of ACAT1 mRNA in all brain regions was observed compared to ACAT2. (B) ACAT1 mRNA after KA injection. (C) ACAT2 mRNA after KA injection. Significant difference compared to controls, by one-way ANOVA with Bonferroni's multiple comparison post-hoc test. * $P<0.05$, ** $P<0.01$.

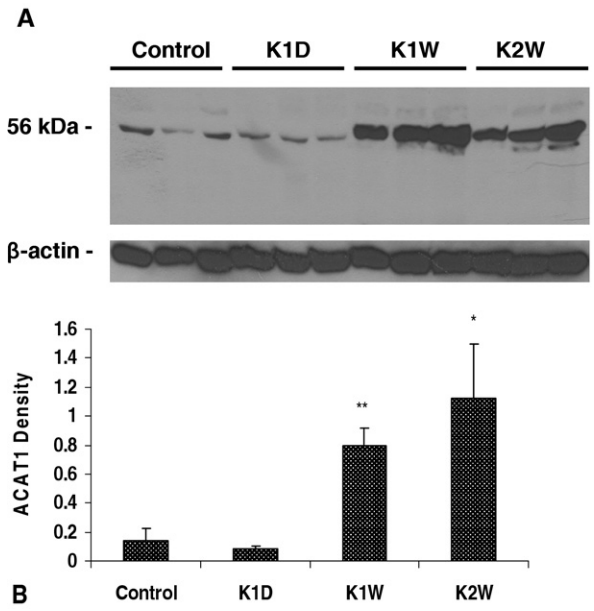

Fig. 2. Western blot analyses of ACAT1. (A) Immunoblot of ACAT1. Lanes 1–3, untreated controls. Lanes 4–6: 1 d post-KA injection. Lanes 7–9: 1 wk post-KA injection. Lanes 10–12: 2 wk post-KA injection. β-actin was used as a loading control. (B) Densitometric analyses of ACAT1 from (A). Significant difference compared to controls, by one-way ANOVA with Bonferroni's multiple comparison post-hoc test. * $P<0.05$, ** $P<0.01$.

the supernatants were lyophilized. The lipid fraction was obtained after drying the supernatants. All samples were kept at −30 °C till analysis. The lipid extracts were reconstituted in 600 μl of $CDCl_3$ containing 0.03% tetramethylsilane (TMS), pipetted into nuclear magnetic resonance (NMR) tubes (5 mm O.D, 7 inch length, Sigma-Aldrich) and the one-dimensional 1H NMR spectra were obtained on a Bruker 800 MHz US 2 spectrometer, operating at 500.15 MHz observation frequency. Lipid extracts were also analyzed using a single 90° pulse, but with no solvent suppression. Typically, 128 scans were collected with 32K data points over a spectra width of 6944 Hz with a relaxation decay of 2 s and an acquisition time of 2.3 s. The 1H NMR spectra were manually processed using TOPSPIN software (Bruker Biospin) and referenced to internal TMS (δ 0.0). Fourier transformed 1H NMR spectra were manually phased and baseline corrected using XWINNMR 3.5 (Bruker Biospin, Rheinstetten, Germany). Each spectrum was integrated between 0.5 and 4.5 and 5.1–10 ppm. To account for any difference in concentration between samples, all data were normalized to a total value of 100. The resulting three-dimensional data, chemical shift, sample name, and relative ion intensity from 1H NMR were analyzed by principal component analysis (PCA). The resulting data were then exported to SIMCA-P+ Software package (Umetrics, Umea, Sweden) for subsequent processing. PCA data were reduced to two latent variables (or principal components, PCs) that describe maximum variation within the data. The PCs obtained from the scores highlighted clustering, trends and outliers in the observation direction in the data set. Statistical analyses of normalized data obtained from 1H NMR were carried out using one-way ANOVA with Bonferroni's multiple comparison post-hoc test ($P<0.05$ was considered significant).

In vitro study of ACAT1 expression in OLN93 oligodendrocytes

OLN93 oligodendrocytes were cultured in DMEM Medium supplemented with 10% fetal bovine serum and 1% penicillin/streptomycin (Gibco, Invitrogen). The cells were plated in 100 mm^2 petri dishes, and maintained in an incubator at 37 °C, 100% humidity, with 95% air, and 5% CO_2. Cells were divided into four groups consisting of untreated controls, KA treatment (100 μM) (He et al., 2009), glutathione monoethyl ester (GSH) (100 μM) (Keller et al., 2000) to increase cellular anti-oxidant level plus KA or phenyl-α-tert-butyl nitrone (PBN) (1 μM) (Hassan et al., 2002) to scavenge free radicals plus KA. All chemicals were dissolved in culture medium. After 1 day of treatment, the cells were harvested to obtain mRNA, and real time

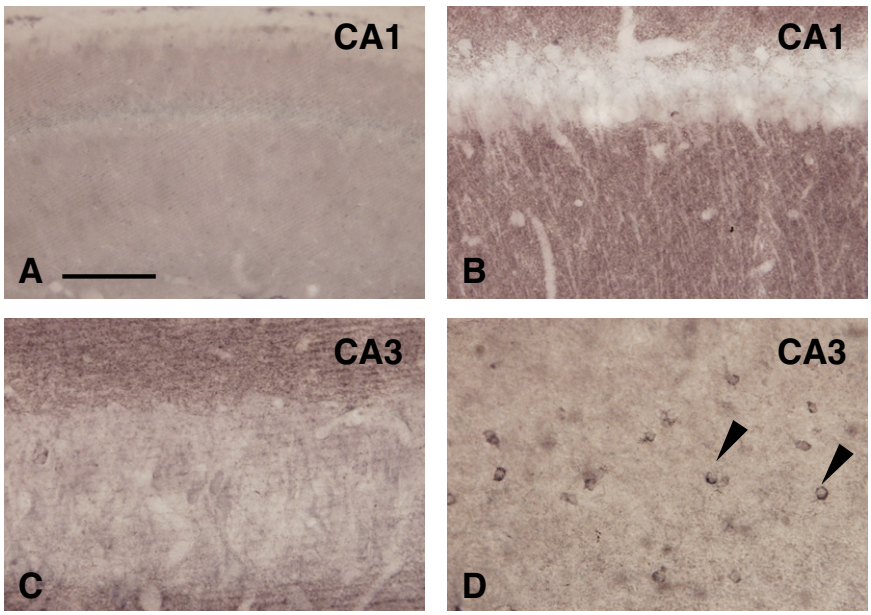

Fig. 3. Immunohistochemical analyses of the hippocampus for ACAT1. (A) Section incubated with antigen absorbed antibody showing absence of labeling. (B) Field CA1 of the normal hippocampus, showing light neuronal labeling for ACAT. (C) Field CA3 of the normal hippocampus. (D) Field CA3 of the hippocampus, 1 wk after KA injection. There is loss of neuronal staining and increased staining in a number of glial cells (arrowheads). Scale=200 μm. For interpretation of the references to color in this figure legend, the reader is referred to the Web version of this article.

RT-PCR was carried out to determine ACAT1 expression. All experiments were carried out in triplicates. Possible significant differences between groups were analyzed using one-way ANOVA with Bonferroni's multiple comparison post-hoc test. $P<0.05$ was considered significant.

RESULTS

RT-PCR analyses

ACAT1 mRNA expression was present throughout the brain, and was highest in the hippocampus. ACAT2 mRNA expression was 1000-fold less than that of ACAT1, confirming a significant difference on expression between ACAT1 and ACAT2 in the brain (Fig. 1A). ACAT1 mRNA level was not significantly different compared to controls at 1 day after KA injection, but increased significantly at 1 week after KA injury (Fig. 1B). The level of ACAT2 generally remained very low after KA injection although minor changes were detected (Fig. 1C).

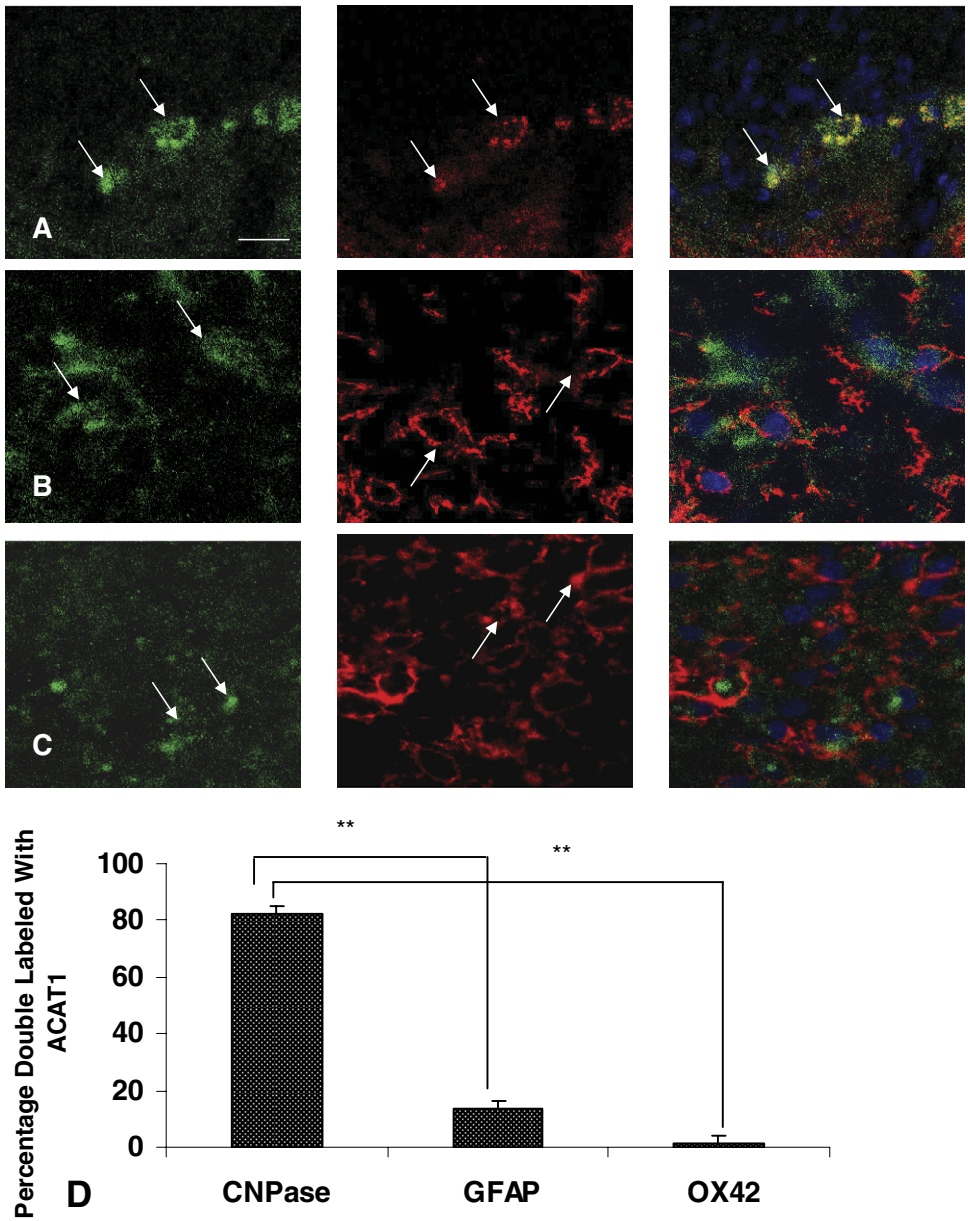

Fig. 4. Double immunofluorescence labeling with antibodies against ACAT1 and CNPase, GFAP, and OX42 of the hippocampus. (A) ACAT1 double labeling with CNPase. Left: ACAT1 staining (arrows). Middle: CNPase staining (arrows). Right: red-green overlap of the antigens shows expression of ACAT1 on oligodendrocytes (arrows). (B) ACAT1 double labeling with GFAP. Left: ACAT1 staining (arrows). Middle: GFAP staining (arrows). Right: no red-green overlap of the antigens. (C) ACAT1 double labeling with OX42. Left: ACAT1 staining (arrows). Middle: OX42 staining (arrows). Right: no red-green overlap of the antigens. Scale=20 μm. (D) Quantification of double labeling of ACAT1 with different glial markers. Significant difference by one-way ANOVA with Bonferroni's multiple comparison post-hoc test. ** $P<0.01$. For interpretation of the references to color in this figure legend, the reader is referred to the Web version of this article.

Western blot analyses

The ACAT1 antibody labeled a band at 56 kDa consistent with the expected molecular weight of the enzyme (Lee et al., 1998) (Fig. 2A). Significantly greater ACAT1 expression was observed after KA lesions compared to controls (Fig. 2B).

Immunoperoxidase labeling

ACAT1 labeling was observed in both white and grey matter regions of the normal brain. White matter tracts such as the corpus callosum and fimbria showed many labeled cells (data not shown). In addition, punctate profiles were labeled in the neuropil of grey matter areas such as the cerebral cortex, hippocampus (Fig. 3A, B), and striatum in the normal brain.

Areas affected by KA lesions showed loss of neurons and dense glial reaction in Nissl stained sections. ACAT1 immunoreactivity was studied at 1 week post-KA injection, since significant change in ACAT1 mRNA and protein was observed at this time. Decreased neuronal staining but increased labeling of glial cells was observed in the grey matter of lesioned CA fields. ACAT1 positive glial cells had small round cell bodies, fine processes, and features of oligodendrocytes (Fig. 3C). Control sections incubated with antigen-absorbed antibody showed absence of staining (Fig. 3D).

Double immunofluorescence labeling

ACAT1 immunoreactivity in the grey matter of the normal hippocampus was localized in punctuate profiles that were not double labeled for CNPase. In contrast, large numbers of oligodendrocytes were observed in the grey matter of the KA lesioned hippocampus, which were double labeled for ACAT1 and CNPase (Fig. 4A). ACAT1 positive cells were not double labeled for GFAP (Fig. 4B) or OX42 (Fig. 4C).

Electron microscopy

The punctate profiles of ACAT1 observed in the grey matter of the hippocampus at light microscopy were found to be axon terminals at electron microscopy. Label was observed in axon terminals that formed asymmetric synaptic contacts with unlabeled dendrites (Fig. 5A, B).

Decreased axonal staining was observed after KA injury. Instead, increased labeling was observed in glial cells with dense heterochromatin and thin rim of dark cytoplasm, characteristic of oligodendrocytes (Fig. 5C).

Serum cholesterol measurement

No significant change in serum cholesterol was observed at any time after KA injury (Fig. 6A).

Gas chromatography-mass spectrometry analyses of the hippocampus

Significantly increased total cholesterol level was detected in the hippocampus, at 1 week and 2 weeks after KA treatment compared to controls (Fig. 6B). Increased levels of COPs were also detected at these times (Fig. 6C) consistent with our previous findings (Kim et al., 2009).

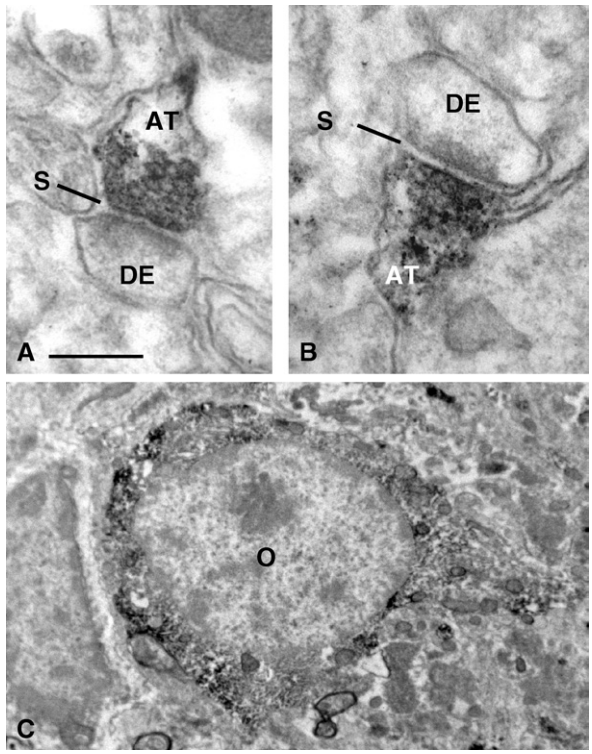

Fig. 5. Electron micrographs of ACAT1 immunolabeled sections of the hippocampus. (A) Axonal label in CA3 region of the control hippocampus. (B) Axonal label in CA1 region of the control hippocampus. (C) Labeled oligodendrocytes (o) in KA treated sections. AT: axon terminal, DE: dendrite, S: synapse. (A, B) Scale=0.2 μm; (C) Scale=0.5 μm.

Nuclear magnetic resonance spectroscopy analyses

Increased level of cholesteryl esters was detected in the hippocampus at 1 week and 2 weeks after KA injection compared to controls. The same result was observed for different species of cholesteryl esters (Fig. 6D). Unlike cholesteryl esters, no significant change in free cholesterol level was detected at these times (Fig. 6E).

In vitro study of ACAT1 expression in OLN93 oligodendrocytes

OLN93 oligodendrocytes showed increased ACAT1 mRNA expression after KA treatment. Cells that had been pre-incubated with GSH did not show this increase (Fig. 7A). Similarly, cells that had been pre-incubated with PBN showed no increase in ACAT1 expression after KA treatment (Fig. 7B).

DISCUSSION

The present study was carried out to elucidate the effect of KA-induced excitotoxic injury on ACAT expression and cholesterol/cholesteryl esters in the rat hippocampus. Ex-

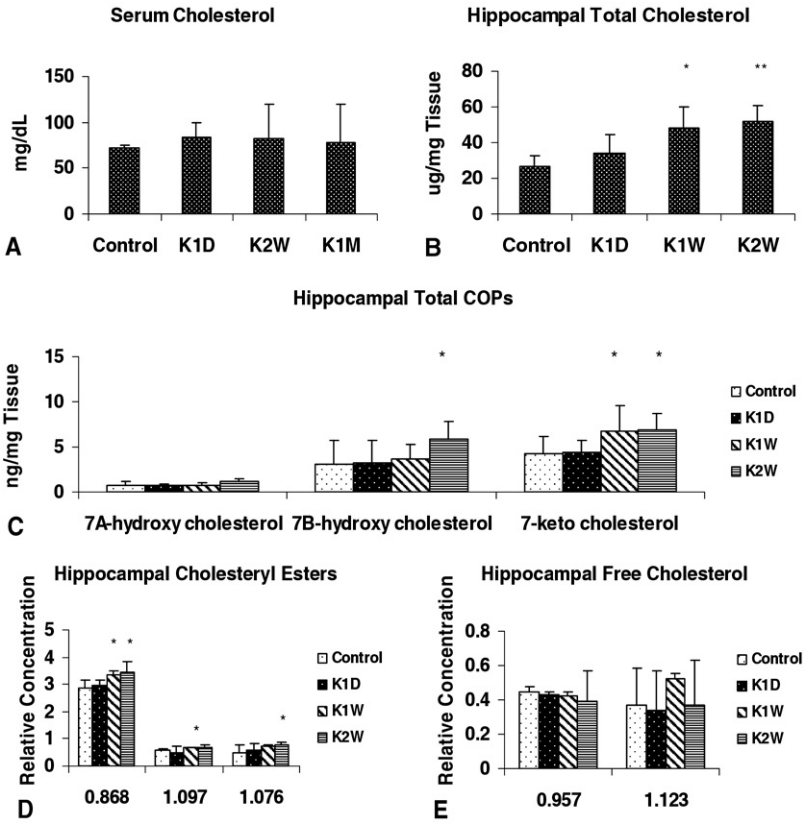

Fig. 6. Serum cholesterol assay (A), gas chromatography-mass spectrometry (B, C), and nuclear magnetic resonance spectroscopy (D, E) analyses of cholesterol, cholesterol oxidation products (COPs), and cholesteryl esters. (A) Serum cholesterol levels. (B) Hippocampal total cholesterol levels. (C) Hippocampal COPs levels. (D) Relative hippocampal cholesteryl ester levels. Significant increase at 1 wk and 2 wk post-KA injection was observed in all species. (E) Relative hippocampal free cholesterol levels. Significant difference compared to controls by one-way ANOVA with Bonferroni's multiple comparison post-hoc test. * $P<0.01$, ** $P<0.01$.

pression of ACAT was first examined in the normal brain. Real time RT-PCR analyses showed that ACAT1 mRNA expression was 1000× greater than ACAT2 in the normal brain, consistent with previous observations that ACAT1 is the major isoform of the enzyme responsible for the cholesteryl ester formation in the brain (Chang et al., 2006). Hence attention was focused on ACAT1 in this study. ACAT1 was found in oligodendrocytes in the white matter consistent with a high level of cholesteryl esters in myelin. In addition, the enzyme was expressed in axons in the normal brain, being localized as punctate profiles in the grey matter of the cerebral cortex and hippocampus. Previous studies have suggested a role of cholesteryl esters in neurite outgrowth, and the growth cone fraction of neurons contains detectable amounts of 22:6-labeled cholesteryl esters (Martin and Bazan, 1992). Non-esterified cholesterol released during terminal breakdown or remodeling is also esterified and transported via apolipoprotein E to neurons undergoing reinnervation, where it is used as a precursor for synthesis of new synapses and terminals (Poirier et al., 1993). Our finding of ACAT1 expression in axons is consistent with recent studies showing expression of a number of genes involved in cholesterol metabolism in neurons (Reviewed in Ong et al., 2010b). Several studies have similarly shown ER localization in axons, although the ER function might be different from that of cell bodies and dendrites (Krijnse-Locker et al., 1995; Weclewicz et al., 1998). Non-specific staining by the ACAT1 antibody is unlikely, since Western blot analysis showed a single band consistent with the expected molecular weight of ACAT1. Control sections incubated with antigen-absorbed antibody showed absence of labeling.

ACAT1 expression and activity were further studied after KA lesions. Areas affected by KA showed neuronal loss and dense glial reaction in Nissl sections indicating neuroinflammation. Non-significant change in ACAT1 mRNA expression of the hippocampus was detected at 1 day, but significant increase in ACAT1 expression was found at 1 week after KA lesions. In contrast to ACAT1, mRNA expression of ACAT2 remained very low after KA treatment. Western blot analysis confirmed that ACAT1 protein expression was increased at 1 and 2 weeks after KA injection. Immunolabeling of KA treated brain sections showed that KA treatment resulted in decreased staining of axon terminals in the neuropil, but increased staining of CNPase positive oligodendrocytes. ACAT1 was mostly not co-expressed in cells that were labeled with the astrocyte or microglial markers, GFAP, and OX42, respectively. Nuclear magnetic resonance spectroscopy confirmed that increased ACAT1 expression is accompanied by increased

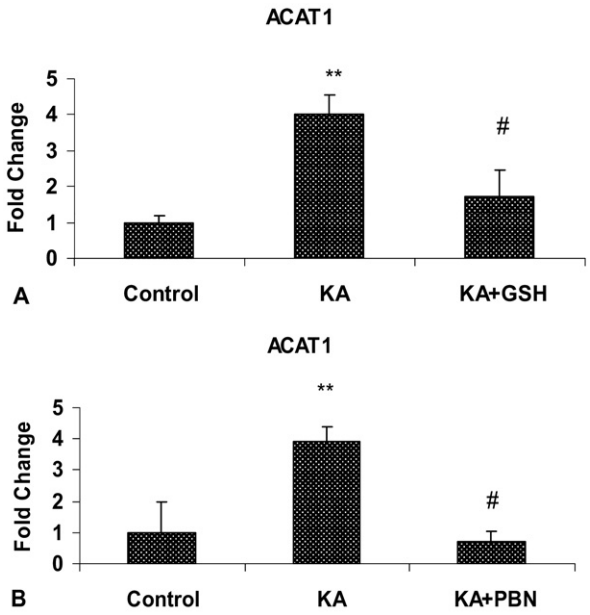

Fig. 7. ACAT1 expression in OLN93 oligodendrocytes. (A) mRNA expression of ACAT1 with KA or KA plus GSH treatment. (B) mRNA expression of ACAT1 with KA or KA plus PBN. Significant difference compared to controls, by one-way ANOVA with Bonferroni's multiple comparison post-hoc test. ** $P<0.01$. Significant difference compared to KA, by one-way ANOVA with Bonferroni's multiple comparison post-hoc test. # $P<0.05$.

levels of cholesteryl esters in the degenerating hippocampus after KA injections, whereas free cholesterol showed no change. A marked elevation (about two-fold) increase in total cholesterol levels was also detected by gas chromatography-mass spectrometry in the lesioned hippocampus at 1 and 2 weeks after KA injection consistent with our previous results (Kim et al., 2009). Serum cholesterol was unaltered after KA lesions. Together, our findings show increased total and esterified cholesterol in degenerating areas affected by KA. In view of observations of increased cholesterol biosynthetic activity in injured neurons (Kim et al., 2009), and evidence of increased arachidonic acid release through elevated phospholipase A_2 activity after KA treatment (Guan et al., 2006; Ong et al., 2010a; Sandhya et al., 1998; Thwin et al., 2003), it is possible that increased ACAT1 activity may be related to the availability of substrates cholesterol and arachidonic acid after neuronal injury.

Previous studies have shown increase in brain cholesteryl esters in brain lesions involving breakdown of myelin. Elevated levels of cholesteryl esters have been detected in brain tissues of patients with multiple sclerosis (Pitkanen et al., 1986) and demyelinating lesions of its animal model, experimental allergic encephalomyelitis (Slavin et al., 1996). Increased cholesteryl esters are also detected in the spinal cord of a mouse model of amyotrophic lateral sclerosis (Cutler et al., 2002). The present study adds to these findings, and demonstrates increased cholesteryl esters in brain areas affected by KA excitotoxicity which spares the white matter. This suggests that increase in cholesteryl esters could be a general feature of neuroinflammation, and not limited to lesions affecting myelinated axons. Increased mRNA levels of ACAT1 and cholesteryl esters are also found in the brain of aged rats (Mulas et al., 2005) and elevated plasma cholesteryl esters levels have been detected in human patients after stroke (Polidori et al., 1998).

ACAT1 inhibition has been used to suppress cholesteryl esters accumulation in experimental studies to treat atherosclerosis (Kogushi et al., 1996; Ooyen et al., 1997) although one study reported that macrophage-specific removal of ACAT1 aggravated atherosclerotic lesions (Fazio et al., 2001). Reduced Aβ plaques formation has also been reported after ACAT1 inhibition (Hutter-Paier et al., 2004; Huttunen and Kovacs, 2008; Puglielli et al., 2001). Increased ACAT1 activity might disrupt membrane cholesterol homeostasis by drawing free cholesterol from plasma membrane during cholesteryl ester synthesis (Bryleva et al., 2010). Conversely, ACAT1 inhibition could lead to increased free cholesterol in cells (Tabas et al., 1996; Warner et al., 1995).

Upregulation of ACAT1 expression was detected in OLN93 oligodendrocytes after KA treatment, and increased expression was prevented by treatment with antioxidant and free radical scavenger *in vitro*. This suggests that ACAT1 expression may be induced by oxidative stress. Several studies have shown that oxidative stress could affect transcription via regulation of nuclear factor kB (Song et al., 2007) and hypoxia inducible factor (Kenneth and Rocha, 2008). Our pilot study on organotypic rat hippocampal cultures showed non-significant improvement in neuronal survival in slices incubated with ACAT1 inhibitor compared to controls after KA treatment (data not shown). Increased cholesteryl ester formation in areas undergoing neuroinflammation could help sequester cholesterol and arachidonic acid, and limit the formation of their toxic oxidation products. On the other hand, cholesteryl esters may be poor substrates of cholesterol efflux pumps compared to free cholesterol, and contribute to total cholesterol buildup in damaged tissues. Further studies are necessary to determine a possible role of ACAT1 in acute and chronic neurodegenerative diseases.

Acknowledgments—This work was supported by grants from the National Medical Research Council to WYO and AMJ (R-181-000-115-275 and R-183-000-155-214/133). We thank Dr. Ya-Jun Wu for help with electron microscopy. ACAT1 inhibitor CP-113,818 was a generous gift from Pfizer.

REFERENCES

Adibhatla RM, Hatcher JF (2008) Altered lipid metabolism in brain injury and disorders. Subcell Biochem 49:241–268.

Alegret M, Llaverias G, Silvestre JS (2004) Acyl coenzyme A:cholesterol acyltransferase inhibitors as hypolipidemic and antiatherosclerotic drugs. Methods Find Exp Clin Pharmacol 26:563–586.

Ben-Ari Y (1985) Limbic seizure and brain damage produced by kainic acid: mechanisms and relevance to human temporal lobe epilepsy. Neuroscience 14:375–403.

Bjorkhem I, Meaney S (2004) Brain cholesterol: long secret life behind a barrier. Arterioscler Thromb Vasc Biol 24:806–815.

Brown AJ, Jessup W (2009) Oxysterols: sources, cellular storage and metabolism, and new insights into their roles in cholesterol homeostasis. Mol Aspects Med 30:111–122.

Brown MS, Ho YK, Goldstein JL (1980) The cholesteryl ester cycle in macrophage foam cells. Continual hydrolysis and re-esterification of cytoplasmic cholesteryl esters. J Biol Chem 255:9344–9352.

Bryleva EY, Rogers MA, Chang CC, Buen F, Harris BT, Rousselet E, Seidah NG, Oddo S, LaFerla FM, Spencer TA, Hickey WF, Chang TY (2010) ACAT1 gene ablation increases 24(S)-hydroxycholesterol content in the brain and ameliorates amyloid pathology in mice with AD. Proc Natl Acad Sci U S A 107:3081–3086.

Chang TY, Chang CC, Ohgami N, Yamauchi Y (2006) Cholesterol sensing, trafficking, and esterification. Annu Rev Cell Dev Biol 22:129–157.

Chang TY, Li BL, Chang CC, Urano Y (2009) Acyl-coenzyme A:cholesterol acyltransferases. Am J Physiol Endocrinol Metab 297: E1–E9.

Cordy JM, Hooper NM, Turner AJ (2006) The involvement of lipid rafts in Alzheimer's disease. Mol Membr Biol 23:111–122.

Cutler RG, Pedersen WA, Camandola S, Rothstein JD, Mattson MP (2002) Evidence that accumulation of ceramides and cholesterol esters mediates oxidative stress-induced death of motor neurons in amyotrophic lateral sclerosis. Ann Neurol 52:448–457.

Fazio S, Major AS, Swift LL, Gleaves LA, Accad M, Linton MF, Farese RV Jr (2001) Increased atherosclerosis in LDL receptor-null mice lacking ACAT1 in macrophages. J Clin Invest 107:163–171.

Folch J, Lees M, Sloane Stanley GH (1957) A simple method for the isolation and purification of total lipides from animal tissues. J Biol Chem 226:497–509.

Guan XL, He X, Ong WY, Yeo WK, Shui G, Wenk MR (2006) Nontargeted profiling of lipids during kainate-induced neuronal injury. FASEB J 20:1152–1161.

Hassan WN, Cantuti-Castelevetri I, Denisova NA, Yee AS, Joseph JA, Paulson KE (2002) The nitrone spin trap PBN alters the cellular response to H(2)O(2): activation of the EGF receptor/ERK pathway. Free Radic Biol Med 32:551–561.

He X, Jenner AM, Ong WY, Farooqui AA, Patel SC (2006) Lovastatin modulates increased cholesterol and oxysterol levels and has a neuroprotective effect on rat hippocampal neurons after kainate injury. J Neuropathol Exp Neurol 65:652–663.

He X, Jittiwat J, Kim JH, Jenner AM, Farooqui AA, Patel SC, Ong WY (2009) Apolipoprotein D modulates F2-isoprostane and 7-ketocholesterol formation and has a neuroprotective effect on organotypic hippocampal cultures after kainate-induced excitotoxic injury. Neurosci Lett 455:183–186.

Hull M, Berger M, Heneka M (2006) Disease-modifying therapies in Alzheimer's disease: how far have we come? Drugs 66:2075–2093.

Hutter-Paier B, Huttunen HJ, Puglielli L, Eckman CB, Kim DY, Hofmeister A, Moir RD, Domnitz SB, Frosch MP, Windisch M, Kovacs DM (2004) The ACAT inhibitor CP-113,818 markedly reduces amyloid pathology in a mouse model of Alzheimer's disease. Neuron 44:227–238.

Huttunen HJ, Kovacs DM (2008) ACAT as a drug target for Alzheimer's disease. Neurodegener Dis 5:212–214.

Keller JN, Huang FF, Dimayuga ER, Maragos WF (2000) Dopamine induces proteasome inhibition in neural PC12 cell line. Free Radic Biol Med 29:1037–1042.

Kenneth NS, Rocha S (2008) Regulation of gene expression by hypoxia. Biochem J 414:19–29.

Kim JH, Jittiwat J, Ong WY, Farooqui AA, Jenner AM (2009) Changes in cholesterol biosynthetic and transport pathways after excitotoxicity. J Neurochem 112:34–41.

Kim JH, Ong WY (2009) Localization of the transcription factor, sterol regulatory element binding protein-2 (SREBP-2) in the normal rat brain and changes after kainate-induced excitotoxic injury. J Chem Neuroanat 37:71–77.

Kogushi M, Tanaka H, Ohtsuka I, Yamada T, Kobayashi H, Saeki T, Takada M, Hiyoshi H, Yanagimachi M, Kimura T, Yoshitake S, Saito I (1996) Anti-atherosclerotic effect of E5324, an inhibitor of acyl-CoA:cholesterol acyltransferase, in Watanabe heritable hyperlipidemic rabbits. Atherosclerosis 124:203–210.

Krijnse-Locker J, Parton RG, Fuller SD, Griffiths G, Dotti CG (1995) The organization of the endoplasmic reticulum and the intermediate compartment in cultured rat hippocampal neurons. Mol Biol Cell 6:1315–1332.

Lee O, Chang CC, Lee W, Chang TY (1998) Immunodepletion experiments suggest that acyl-coenzyme A:cholesterol acyltransferase-1 (ACAT-1) protein plays a major catalytic role in adult human liver, adrenal gland, macrophages, and kidney, but not in intestines. J Lipid Res 39:1722–1727.

Leon C, Hill JS, Wasan KM (2005) Potential role of acyl-coenzyme A:cholesterol transferase (ACAT) inhibitors as hypolipidemic and antiatherosclerosis drugs. Pharmacol Res 22:1578–1588.

Leoni V, Lutjohann D, Masterman T (2005) Levels of 7-oxocholesterol in cerebrospinal fluid are more than one thousand times lower than reported in multiple sclerosis. J Lipid Res 46:191–195.

Livak KJ, Schmittgen TD (2001) Analysis of relative gene expression data using real-time quantitative PCR and the 2(-Delta Delta C(T)) method. Methods 25:402–408.

Ma MT, Zhang J, Farooqui AA, Chen P, Ong WY (2010) Effects of cholesterol oxidation products on exocytosis. Neurosci Lett 476: 36–41.

Martin RE, Bazan NG (1992) Changing fatty acid content of growth cone lipids prior to synaptogenesis. J Neurochem 59:318–325.

Mulas MF, Demuro G, Mulas C, Putzolu M, Cavallini G, Donati A, Bergamini E, Dessi S (2005) Dietary restriction counteracts age-related changes in cholesterol metabolism in the rat. Mech Ageing Dev 126:648–654.

Nadler JV, Perry BW, Cotman CW (1978) Intraventricular kainic acid preferentially destroys hippocampal pyramidal cells. Nature 271: 676–677.

Ong WY, Farooqui T, Farooqui AA (2010a) Involvement of cytosolic phospholipase A(2), calcium independent phospholipase A(2) and plasmalogen selective phospholipase A(2) in neurodegenerative and neuropsychiatric conditions. Curr Med Chem 17:2746–2763.

Ong WY, Goh EW, Lu XR, Farooqui AA, Patel SC, Halliwell B (2003) Increase in cholesterol and cholesterol oxidation products, and role of cholesterol oxidation products in kainate-induced neuronal injury. Brain Pathol 13:250–262.

Ong WY, Kim JH, He X, Chen P, Farooqui AA, Jenner AM (2010b) Changes in brain cholesterol metabolome after excitotoxicity. Mol Neurobiol 41:299–313.

Ooyen C, Zecca A, Zanelli T, Catapano AL (1997) Decreased intracellular degradation and increased secretion of apo B-100 in Hep G2 cells after inhibition of cholesteryl ester synthesis. Atherosclerosis 130:143–152.

Pitkanen AS, Halonen TO, Kilpelainen HO, Riekkinen PJ (1986) Cholesterol esterase activity in cerebrospinal fluid of multiple sclerosis patients. J Neurol Sci 74:45–53.

Poirier J, Baccichet A, Dea D, Gauthier S (1993) Cholesterol synthesis and lipoprotein reuptake during synaptic remodelling in hippocampus in adult rats. Neuroscience 55:81–90.

Polidori MC, Frei B, Cherubini A, Nelles G, Rordorf G, Keaney JF Jr, Schwamm L, Mecocci P, Koroshetz WJ, Beal MF (1998) Increased plasma levels of lipid hydroperoxides in patients with ischemic stroke. Free Radic Biol Med 25:561–567.

Puglielli L, Konopka G, Pack-Chung E, Ingano LA, Berezovska O, Hyman BT, Chang TY, Tanzi RE, Kovacs DM (2001) Acyl-coenzyme A: cholesterol acyltransferase modulates the generation of the amyloid beta-peptide. Nat Cell Biol 3:905–912.

Racine RJ (1972) Modification of seizure activity by electrical stimulation. II. Motor seizure. Electroencephalogr Clin Neurophysiol 32: 281–294.

Rudel LL, Lee RG, Cockman TL (2001) Acyl coenzyme A: cholesterol acyltransferase types 1 and 2: structure and function in atherosclerosis. Curr Opin Lipidol 12:121–127.

Sandhya TL, Ong WY, Horrocks LA, Farooqui AA (1998) A light and electron microscopic study of cytoplasmic phospholipase A2 and cyclooxygenase-2 in the hippocampus after kainate lesions. Brain Res 788:223–231.

Slavin DA, Bucher AE, Degano AL, Soria NW, Roth GA (1996) Time course of biochemical and immunohistological alterations during experimental allergic encephalomyelitis. Neurochem Int 29:597–605.

Song YS, Lee YS, Narasimhan P, Chan PH (2007) Reduced oxidative stress promotes NF-kappaB-mediated neuroprotective gene expression after transient focal cerebral ischemia: lymphocytotrophic cytokines and antiapoptotic factors. J Cereb Blood Flow Metab 27:764–775.

Tabas I, Marathe S, Keesler GA, Beatini N, Shiratori Y (1996) Evidence that the initial up-regulation of phosphatidylcholine biosynthesis in free cholesterol-loaded macrophages is an adaptive response that prevents cholesterol-induced cellular necrosis. Proposed role of an eventual failure of this response in foam cell necrosis in advanced atherosclerosis. J Biol Chem 271:22773–22781.

Thwin MM, Ong WY, Fong CW, Sato K, Kodama K, Farooqui AA, Gopalakrishnakone P (2003) Secretory phospholipase A2 activity in the normal and kainate injected rat brain, and inhibition by a peptide derived from python serum. Exp Brain Res 150:427–433.

Turkish AR, Sturley SL (2009) The genetics of neutral lipid biosynthesis: an evolutionary perspective. Am J Physiol Endocrinol Metab 297:E19–E27.

Warner GJ, Stoudt G, Bamberger M, Johnson WJ, Rothblat GH (1995) Cell toxicity induced by inhibition of acyl coenzyme A:cholesterol acyltransferase and accumulation of unesterified cholesterol. J Biol Chem 270:5772–5778.

Weclewicz K, Svensson L, Kristensson K (1998) Targeting of endoplasmic reticulum-associated proteins to axons and dendrites in rotavirus-infected neurons. Brain Res Bull 46:353–360.

Zhang J, Xue R, Ong WY, Chen P (2009) Roles of cholesterol in vesicle fusion and motion. Biophys J 97:1371–1380.

Zhang Y, Yu C, Liu J, Spencer TA, Chang CC, Chang TY (2003) Cholesterol is superior to 7-ketocholesterol or 7 alpha-hydroxycholesterol as an allosteric activator for acyl-coenzyme A:cholesterol acyltransferase 1. J Biol Chem 278:11642–11647.

Zhao XQ, Krasuski RA, Baer J, Whitney EJ, Neradilek B, Chait A, Marcovina S, Albers JJ, Brown BG (2009) Effects of combination lipid therapy on coronary stenosis progression and clinical cardiovascular events in coronary disease patients with metabolic syndrome: a combined analysis of the Familial Atherosclerosis Treatment Study (FATS), the HDL-Atherosclerosis Treatment Study (HATS), and the Armed Forces Regression Study (AFREGS). Am J Cardiol 104:1457–1464.

(Accepted 8 April 2011)
(Available online 14 April 2011)